Available online at www.sciencedirect.com
SCIENCE DIRECT
Polymer 46 (2005) 8883–8891
polymer
www.elsevier.com/locate/polymer

IR spectroscopic investigation of the effect of deep UV irradiation on PET films

Zhengmao Zhu[a], Michael J. Kelley[a,b,*]

[a]Department of Applied Science, College of William and Mary, P.O. Box 8795, Williamsburg, VA 23187, USA
[b]Jefferson Lab, Free Electron Laser Department, 12000 Jefferson Ave, Newport News, VA 23606, USA

Received 14 October 2004
Available online 23 June 2005

Abstract

Infrared spectroscopy provides a comprehensive view of chemical and conformational structures of molecules. Spin cast amorphous and semicrystalline PET thin films on silicon substrates were investigated with transmission IR to reveal the effect of deep UV (172 nm) irradiation on molecular architecture. Difference spectra by subtracting original samples from the UV treated ones show features consistent with a Norrish type I based decarbonylation and a Norrish type II process producing terminal carboxylic acid groups. Conformation selectivity of the photochemistry is discussed on the basis of three major structure factors related to the formation of a cyclic transition state of the Norrish type II process. Quantitative analysis was carried out by simulating carbonyl stretching band in the difference spectra with ester and acid type carbonyl model spectra. The effects of UV fluence and molecular mobility on quantum yields were elucidated. Quantum yields of 172 nm UV photochemistry in bulk PET were calculated to be no different from those of longer wavelength (200–400 nm). UV modified depth were also estimated by means of plasma etching of the samples.

Keywords: Infrared spectroscopy; Polymer photochemistry; Thin film

1. Introduction

The enormous scale of PET fiber production—more than 8.3 million metric tons in 2002 [1]—makes it an attractive target for environmentally friendly surface modification by UV photochemistry. Earlier studies of UV-induced photodegradation provide a starting point. Day and Wiles [2–5] used xenon or carbon arc sources and high pressure mercury lamps (200–400 nm) under nitrogen purge or vacuum, finding CO and carboxylic acid production as the major effects, attributing the former mainly to a Norrish type I process followed by decarbonylation:

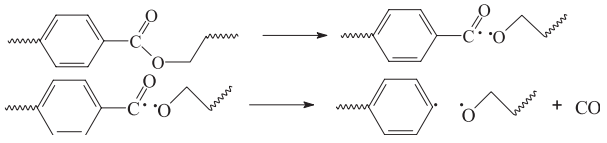

and the latter to a Norrish type II process involving a cyclic six-membered transition state:

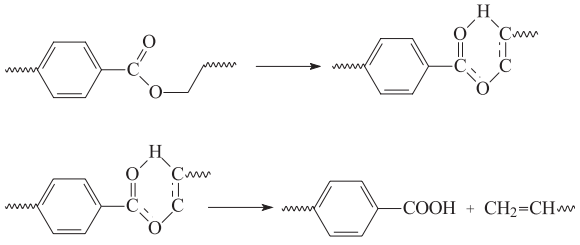

Others later reported the effect of 185 nm (low-pressure mercury discharge) [6], 193 nm (ArF* laser) [7], or 222 nm (KrCl* excimer lamps) [8,9] and details of their findings are discussed in Ref. [10].

We recently reported [10] the effect of 172 nm irradiation (Xe excimer lamp) under continuous nitrogen purge on PET surface composition. XPS analysis of these

* Corresponding author. Address: Jefferson Lab, Free Electron Laser Department, 12000 Jefferson Ave, Newport News, VA 23606, USA. Tel.: +1 757 269 5736; fax: +1 757 269 5755.
E-mail address: mkelley@jlab.org (M.J. Kelley).

0032-3861/$ - see front matter © 2005 Elsevier Ltd. All rights reserved.
doi:10.1016/j.polymer.2005.05.135

materials showed CO elimination and acid functional group creation (as evidenced by silver derivatization) increasing with fluence up to 16 J/cm^2. In addition, ToF/SIMS analysis of these materials [11] found the same fluence dependence of terephthalic acid type polymer end group and carbonyl deficient structure formation, providing further support for Norrish type I and Norrish type II mechanisms. However, the depth of transformation exceeds the probe depth of ToF/SIMS and XPS, limiting their usefulness for determining the quantum yields.

Infrared spectroscopy can be a very powerful tool for studying chemical structure in bulk materials as well as providing molecular conformation details that are inaccessible to most analytical methods. There are numerous reports [12–24] of its application to PET. Three structure factors are essential to the conformation of a PET molecule: rotation of the carbonyl groups about the C_{ar}–CO or CO–O bonds, *gauche* (*G*) or *trans* (*T*) forms of the glycol C–C bonds, and the *gauche* (*g*) or *trans* (*t*) conformers resulting from rotation about the C–O bonds of the glycol linkage. PET is present in an almost planar conformation in the crystalline state: two carbonyl bonded adjacent to each benzene ring lies in the plane with *trans* arrangement with respect to each other, and all *trans* (*Tt*) conformations with respect to C–C and C–O bonds, according to X-ray diffraction analysis [25], whilst additional conformers exist in amorphous and drawn samples. The interpretation of chemical and conformational origin of most PET infrared peaks is well established based on the assignments proposed by Boerio et al. [19,20] and those of Miyake [14,15]. Accordingly, IR spectroscopy offers an important view of the effect of deep UV light on the molecular architectures. In turn, the knowledge of photochemistry can serve as a useful probe into the structure and molecular dynamics of solid polymers and may deepen the understanding of IR spectroscopy.

2. Experimental section

2.1. PET film preparation

PET solutions of 1–8% concentration in *o*-chlorophenol were prepared by dissolving small pieces of the untreated DuPont Mylar® LB 48 film used in our previous work. They were spin cast onto polished silicon wafers with CHEMAT Technology spin coater to acquire uniform films of 70–500 nm thickness. Heating in a vacuum oven at ~70 °C for 2 h yielded solvent-free amorphous films. Half of each was cleaved off and heated in the vacuum oven at ~200 °C for another 2 h to thermally crystallize the film to produce semicrystalline PET.

Film thickness was measured directly as the step height of knife-cut trench through it. Step height measurements by Dektak^3 ST surface profiler and by 'NanoScope® IV' scanning probe microscope were in good agreement, but the latter provided better precision (~ ±2 nm). The scanning probe microscope was operated in intermittent contact ('tapping') mode with low module (15 mN/m) silicon tip at 0.25 Hz to scan over multiple 60×8 μm^2 sampling areas across the film/substrate step edge.

2.2. Excimer lamp exposures

The UV irradiations were accomplished with a dielectric barrier discharge (DBD) excimer lamp of our own construction, as described in the earlier report [10]. The lamp is enclosed within a coaxial polycarbonate cylinder, sealed at the ends and continuously swept by boil-off from liquid nitrogen. The material to be treated was attached to the inner surface of the enclosure, providing a constant distance to the lamp of about 7 cm. The irradiance at the sample position was measured with an International Light Model 1400A photometer with a SED-185 detector head. The spectral energy distribution of the lamp and the detector response curve do not overlap perfectly, necessitating a correction factor of 2 to the meter reading to obtain the UV dose. Average irradiance received at sample position is about 50 mW/cm^2. All films were exposed to 8 J/cm^2 UV simultaneously and removed for analysis. Another two exposures of 8 J/cm^2 UV dose to the same set of samples led to total dose of 16 and 24 J/cm^2. IR spectra were collected after each run. Sample surface temperature was monitored by thermocouple readout and remained lower than 60 °C.

2.3. Air plasma etching

Plasma etching was carried out by Hummer 6.2 sputtering system under the plasma mode at 60 mTorr dry air and 6 mA current. The measured average etching rate on PET polymer was about 1 nm/s but negligible on silicon substrate. After every ~10 s etching, samples were removed for IR and (or) AFM analysis.

2.4. IR spectra measurement

IR spectra between 4000 and 400 cm^{-1} were acquired by transmission FTIR with Thermo Nicolet Nexus 760 at 4 cm^{-1} resolution (100 summations) using a DTGS detector. The silicon supported thin films were mounted with a magnetic film holder using (1/4) in. by (1/2) in. slot at normal incidence of the IR beam. Sample positions were marked and preserved throughout the experiment. Monomethyl terephthalate (Fluka, >97%) and dimethyl terephthalate (Alfa Aesar, 99%) were dissolved separately in chloroform (Certified A.C.S.) to make 10^{-2} mol/L solutions. Solution spectra were gathered with NSG Precision Cells of 0.5 mm path-length with CaF_2 windows.

3. Results and discussion

3.1. Unirradiated films

IR spectra show typical absorption bands of amorphous or semicrystalline PET (Fig. 1) similar to those documented in the literature, except for the variation of the background due to film thickness dependent optical effects caused by reflections from polymer surface and polymer/substrate interface [26]. A first step is to verify that Lambert–Beer law still holds for these samples. The 1410 cm^{-1} in-plane ring mode is generally believed to be insensitive to molecular chain conformation [27], making it a good reference to test absorbance-thickness relationship. Fig. 2 shows a good linear relationship between the peak area at 1410 cm^{-1} and the thickness of amorphous films. For semicrystalline films, a somewhat different background in 1410 cm^{-1} absorption band area may have caused the band intensity to be seemingly lower (~5%). Nevertheless we can reasonably apply Lambert–Beer law for these materials.

Using 1410 cm^{-1} band as the thickness reference provides a way to normalize spectral intensities among materials. The mode at ~1340 cm^{-1} (–CH_2– wagging) originates from *trans* glycol segment [20], making 1340 cm^{-1}/1410 cm^{-1} peak ratio a good indication of the *trans* glycol content. Fig. 3(a) shows higher *trans* conformation content, thus extended structures, in thinner films than thicker ones though all were prepared under the same parameters except for different solution concentration. Especially, there was a dramatic increase of *trans* content when film thickness is smaller than about ~200 nm. Much the same information is revealed with depth profiling by air plasma etching of a 500 nm film (Fig. 3(b)). The plasma etching process causes a damage zone of less than 5 nm depth and, therefore, will not significantly alter the information obtained [28]. Increasingly extensive etching shows an increasing amount of *trans* conformation closer to the PET/silicon interface, especially in the region less than ~200 nm from the interface. These results indicate that the molecular conformation varied with film thickness as well as with depth of the same film, attributable to the shear stress that molecules experienced during film formation [29–31]. Thermal annealing is inadequate to relax shear-induced structural anisotropy in confined polymer systems because of insufficient mixing at the interface [30]. We found a similar conformation-thickness relationship in the thermally crystallized films. According to Sills et al. [29], the shear induced structuring results in an elevated glass transition temperature and hence low molecular mobility due to the high residual internal stress after annealing. In addition, favorable film-substrate interaction would also lead to lower molecular mobility in vicinity of polymer-substrate interface [32,33]. Accordingly, correct interpretation of the effect of UV irradiation on films of different thickness must take into account the low molecular mobility region.

3.2. UV modified films

One hundred and seventy-two nanometer UV is strongly absorbed by PET so that the majority of photochemical transformation occurs in a thin near surface layer, which makes it difficult to detect in transmission spectra from freestanding films (a few microns thick) with vibrational spectroscopy. While attenuated total reflectance IR can be used to look at sub-micron near surface layers in polymers, the difficulty in maintaining repeatable optical contact between polymer film and internal reflection element necessitates the use of a depth reference band [27]. A suitable choice is uncertain for photochemical modification studies, as we will show most PET IR absorption bands are correlated and affected by UV irradiation. Such

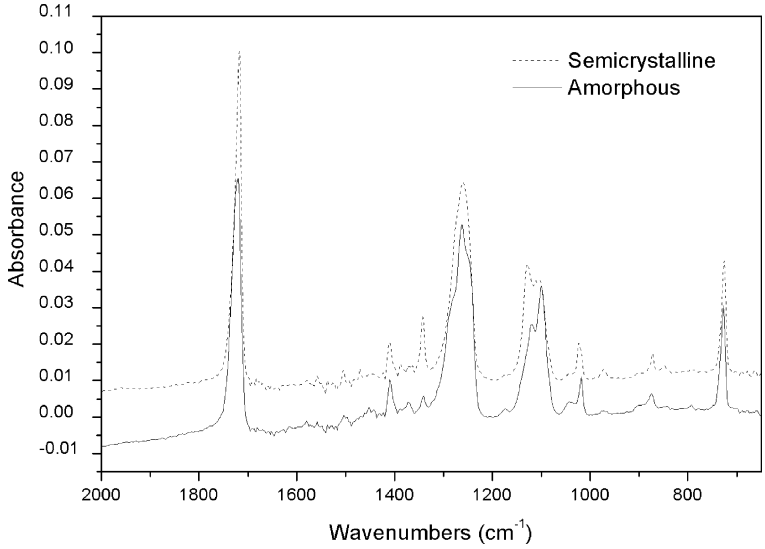

Fig. 1. IR spectra of ~140 nm thick semicrystalline and amorphous PET films.

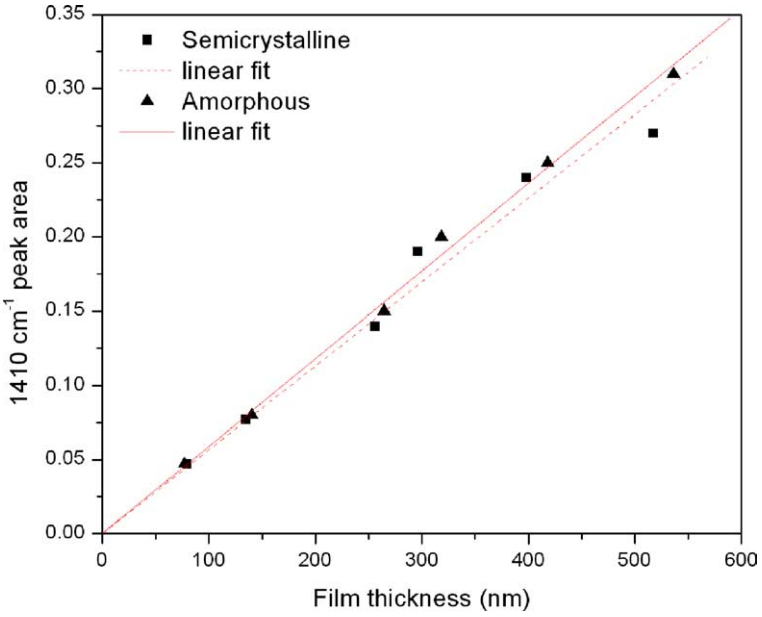

Fig. 2. Linear correlations between the peak area at 1410 cm^{-1} and the thickness of PET films.

complications do not attend transmission FTIR of silicon supported thin films.

The spectral differences between the UV treated films and untreated ones are not obvious in overplots. This is due to the very low quantum yield brought about by the rigidity of the solid matrix. Longer exposure time will provide somewhat higher concentration of photodegradation product for analysis, but photooxidation may complicate the results [5]. Fortunately, the excellent data quality makes possible spectral subtraction, which proves revealing. Fig. 4 displays the difference spectra obtained by subtracting spectra of ~140 nm amorphous and semi-crystalline films from those of the respective 8 J/cm^2 UV treated ones (we will refer to these spectra as difference spectra without explicitly mentioning the reference spectra throughout the article for simplicity). Most noticeable is the negative absorbance at the positions close to major PET IR bands (summarized in Table 1) [14,20,24], C=O stretching at about 1720 cm^{-1} (~1721 cm^{-1} for amorphous samples and ~1716 cm^{-1} for semi-crystalline samples), ring in plane deformation at ~1410 cm^{-1}, –CH_2– wagging at ~1340 cm^{-1}, ring and ester modes at 1300–1000 cm^{-1},

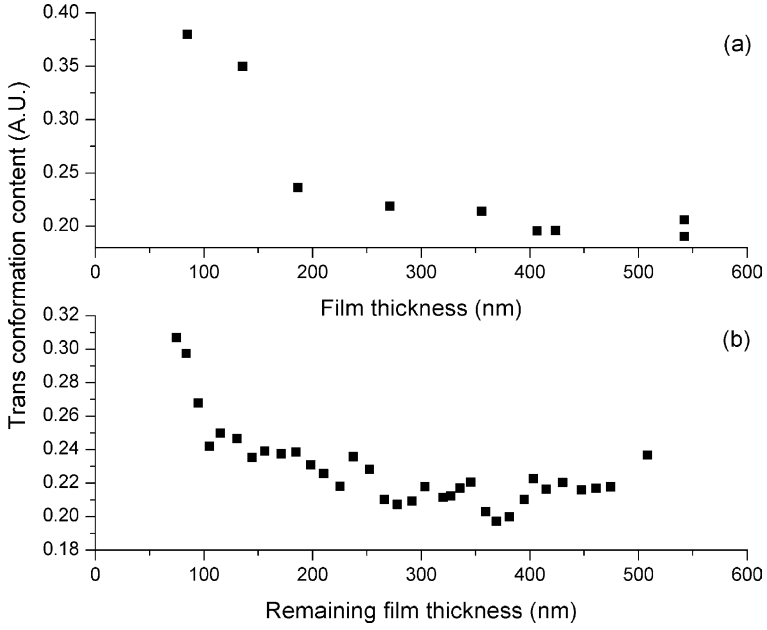

Fig. 3. (a) *trans* Conformation content of spin cast amorphous PET films. (b) Conformation profile generated by plasma removal of surface layers from a 500 nm spin cast amorphous PET film.

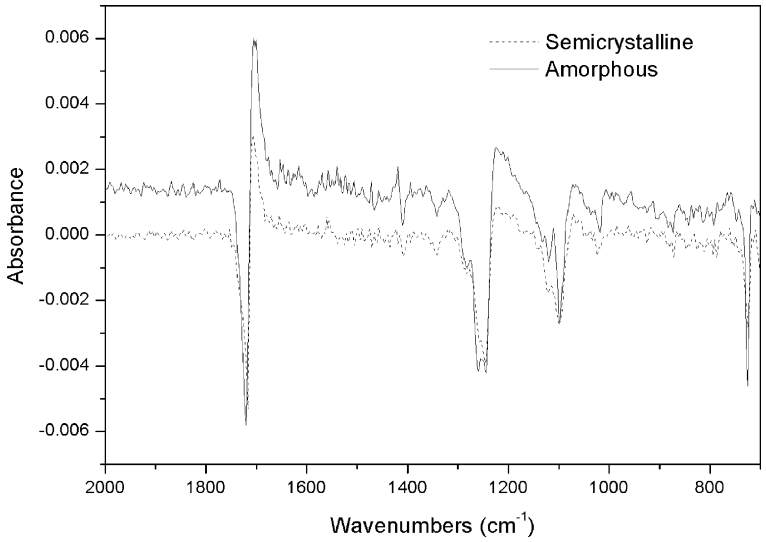

Fig. 4. Difference spectra produced by subtracting spectra of ~140 nm amorphous and semi-crystalline PET films from those of the respective 8 J/cm^2 UV treated ones.

and ring C–H+C=O out of plane bending at ~725 cm^{-1} along with strong positive absorbance band at ~1700 cm^{-1} and two broad poorly defined positive absorbance band at ~1220 and ~1070 cm^{-1}. Since AFM detected no reduction of thickness of any samples after up to 24 J/cm^2 UV dose irradiation, these variations should be attributed to photochemically induced molecular structure changes.

Interpretation of PET IR spectra in general is non-trivial, even more so those of UV treated specimens, as the potential energy distributions of various vibration modes are rather complicated [20]. The assigned carbonyl-stretching band is one of few relative pure normal modes and thus may be interpreted to be the result of transformations directly related with the carbonyl groups. The negative peak observed at close to the original carbonyl stretching peak positions can be attributed to loss of those carbonyl functional groups whereas the positive peak appeared at slightly lower wave number should correspond to new type(s) of carbonyl functional groups created. These may be carboxylic acids, as acid type carbonyl stretching is known to show up at slightly lower wavenumber than corresponding ester type carbonyl. These findings are consistent with previous surface analysis of 172 nm UV treated PET, finding carbonyl elimination and acid creation the major photochemical results [10,11]. The carbonyl elimination will cause other negative peaks since the carbonyl group is a part of the ester group and a substituent group of the phenylene ring. To some degree, all ester modes, ring modes would be affected by the loss of carbonyl. The acid creation may also be responsible for some of the negative peaks such as ester modes at 1300–1000 cm^{-1} and –CH_2– wagging mode of *trans* glycol groups at 1340 cm^{-1} with the breaking of CH_2–O bond.

Relating the photochemistry to molecular conformation in different morphology provides further insight. The Norrish type II reaction has to proceed through a cyclic six-membered transition state, which requires *trans* (*T*) glycol conformation and a *gauche* (*g*) conformation with respect to the CH_2–O bonds of the glycol linkage, as well as some degree of carbonyl rotation (Fig. 5) to facilitate the 'in-plane' *n*-orbital-initiated intramolecular hydrogen abstraction [34]. Since UV treatments were conducted

Table 1
Major peak positions in the difference spectra between 8 J/cm^2 UV treated and untreated ~140 nm PET films and assignments based on original PET IR band

Amorphous sample	Semicrystalline sample	Corresponding PET band
1721[a]	1716[a]	C=O stretch
1410	1408	Ring in-plane def
1342	1342	CH_2 wagging (*trans*)
1282	1282	Ring-ester in-plane mode
1259	1257	Ring-ester in-plane mode
1244	1246	Ring-ester in-plane mode
1120	1122	Ring-ester in-plane mode
1099	1099	Symmetric glycol C–O stretch (*gauche*)
1018	1024	Ring C–H in-plane def
725	725	Ring C–H+C=O out-of-plane def

[a] Not the exact peak position due to differential peak shape.

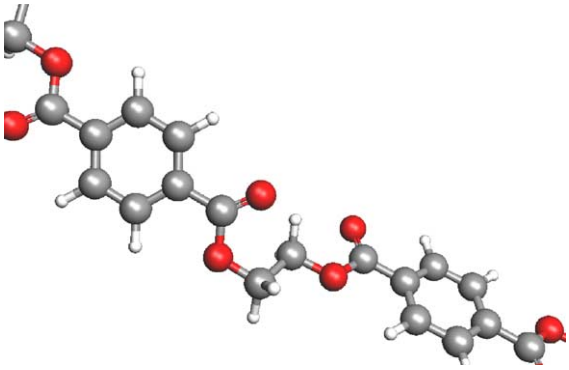

Fig. 5. Pictorial view of possible cyclic six-membered transition state conformation.

below glass transition temperature of PET so that available polymer movement is limited, the difference spectra may reflect some of the conformation preference.

Consider PET conformation in terms of above three structural factors. First, the *gauche* (*G*) or *trans* (*T*) conformation of the ethylene glycol fragment through rotation about C–C bond accounts for major IR spectra differences in amorphous and crystalline. The idea has now been widely accepted since first proposed by Ward [12]. Its vibration modes were extensively studied [14,19]: e.g. the 1340 cm^{-1} band assigned to $–CH_2–$ wagging of *trans* (*T*) glycol groups, primary found in crystalline phase, and 1370 cm^{-1} band for *gauche* (*G*) form in amorphous phase. Interestingly, the *gauche* (*G*) mode at 1370 cm^{-1} was not evident in the difference spectra between 8 J/cm^2 UV treated and untreated films whilst the *trans* (*T*) mode at 1340 cm^{-1} was well resolved, even though both were about the same intensity in the spectra of untreated amorphous films. This suggests the dominance of a photochemical reaction that selectively affects *trans* glycol conformer, consistent with the *trans* (*T*) conformation requirement of Norrish type II transition state.

Second, the conformation with respect to the dihedral angle about CH_2–O bond was also deemed important [22] but its assignment to certain IR bands is still ambiguous. Miyake [14] assigned the band at 1099 cm^{-1} to symmetric stretching of *gauche* (*g*) C–O form whereas Cole et al. [24] related this mode to 1092 cm^{-1} band. We observed the 1099 cm^{-1} to be the dominant band in the 1200–1000 cm^{-1} range of both amorphous and semicrystalline difference spectra (Fig. 4) but different prominence in the original spectra (Fig. 1). As the Norrish type II process is the dominant process (shown in later sections), this finding supports Miyake's assignment. In addition, comparisons between peak intensities of the difference spectra at ~1042 cm^{-1} (*gauche* C–O asymmetric stretching) and ~973 cm^{-1} (*trans* C–O asymmetric stretching) suggest little photochemical preference of *gauche* (*g*) form to *trans* (*t*) form.

The third conformation factor for the PET molecule involves the rotation of the carbonyl groups about the C_{ar}–CO bond, affecting the carbonyl peak position and shape [24]. The carbonyl conformations in amorphous films are in a disordered state with respect to the planes of the benzene ring and the corresponding carbonyl stretching band is relatively broad (FWHM ~24 cm^{-1}) and centered at 1724 cm^{-1} whereas carbonyl groups are more ordered in the semicrystalline film as reflected by narrower stretching band (FWHM ~18 cm^{-1}, centered at 1718 cm^{-1}). The carbonyl-stretching band of the difference spectra in either semicrystalline or amorphous has a negative absorbance portion closely resembling the carbonyl peak of the respective untreated samples (inverted). The UV transformed carbonyl bands are representative of their morphology. This suggests that photochemical transformation of carbonyl groups does not favor either particular carbonyl conformation or morphology. The low conformation selectivity may be because the low rotation barrier of the C_{ar}–CO bond [35] can be easily overcome by photo-excited molecules.

In principle, quantitative analysis of carboxylic acid and decarbonylation yields is possible by numerically resolving the differential carbonyl peak into a combination of positive and negative carbonyl bands. However, this numerical approach is not sufficiently stable due to the differential peak shape, complex individual carbonyl band, and low signal level. An alternative is simulation of the differential carbonyl band with a linear combination of model spectra of ester and carboxylic acid carbonyls. First, as previously discussed, the negative carbonyl band strongly resembles spectra of untreated PET (inverted), suggesting them as models for the negative portion. Second, the photolytically produced carboxylic acid has a band position independent of PET morphology and the polymer end carboxylic acid structure resembles that of mono-methyl terephthalate or mono-ethyl terephthalate. The acid type carbonyl spectrum were modeled by the spectra subtraction result of mono-methyl terephthalate chloroform solution spectrum (10^{-2} M) and one-half intensity of dimethyl terephthalate chloroform solution spectrum (10^{-2} M) so that the resulting carbonyl band is a comprehensive representative of the acid carbonyl and its possible influence on the opposite ester carbonyl. The carbonyl band area of this acid model spectrum is about 1.31 times of that of same amount of carbonyl groups in dimethyl terephthalate, which must be accounted for in quantitative analysis. Simulation of the difference spectra was performed by linear least square fitting with these contributions in the 1624–1857 cm^{-1} range along with a linear background correction. Fig. 6 shows excellent agreements of the difference spectra of 8 J/cm^{-1} treated ~140 nm thick amorphous and semicrystalline films with the corresponding simulated linear least square fit spectra. Excellent matches were also observed between other difference spectra and the simulated ones, supporting the legitimacy of the approach. Following data interpretations are based on spectra fitting results of acid carbonyl band area, related to the amount of acid product, and the ester

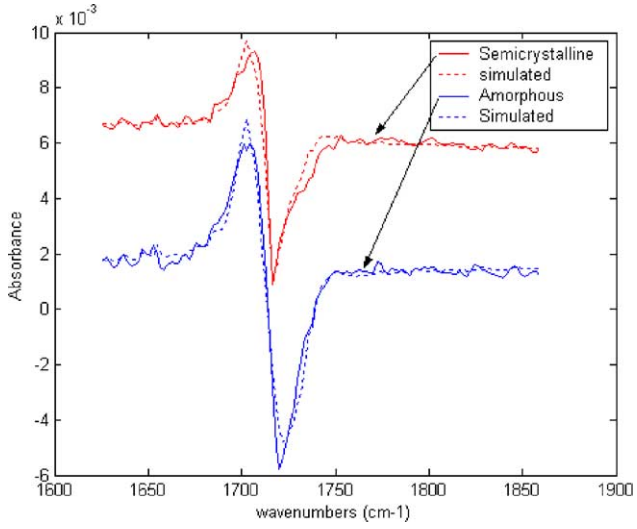

Fig. 6. Comparison of the difference spectra of 8 J/cm^{-1} treated ~140 nm semicrystalline and amorphous PET with the respective simulated linear least square fit spectra.

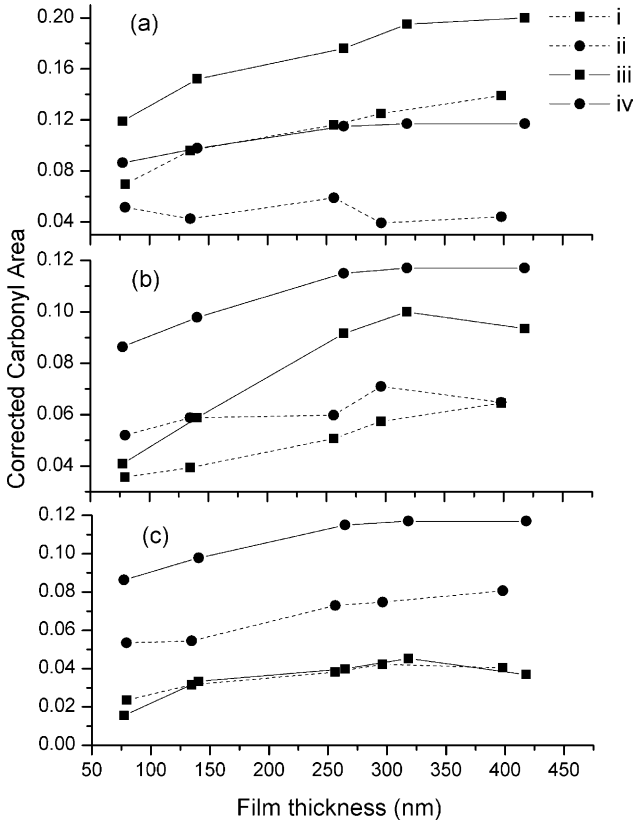

Fig. 7. Acid and decarbonylation yields (in terms of carbonyl band areas) from (a) the first, (b) the second, and (c) the third 8 J/cm^2 UV exposures to amorphous and semicrystalline samples of various thickness. (i) Acid production in semicrystalline PET (ii) decarbonylation in semicrystalline PET (iii) acid production in amorphous PET (iv) decarbonylation in amorphous PET.

type carbonyl band area, to the total number of transformed carbonyl groups.

Fig. 7(a) summarizes the effect of the first 8 J/cm^2 UV dose exposure on amorphous and semicrystalline samples of various thickness in terms of carbonyl areas, corrected for the molar absorptivity difference between acid and ester carbonyl (in ester type). At a particular sample thickness, where a pair of amorphous and semicrystalline samples were made out of the same spin cast film and the semicrystalline one was slightly thinner because of the higher density (5–7%), much higher yields of both Norrish type I and type II products were observed for the amorphous samples than their semicrystalline counterparts. We attribute this to the higher density of semicrystalline films and hence the lower molecular chain mobility than that in amorphous films. It is also apparent that the acid production dominated the decarbonylation process at this dose level. While comparing films of different thickness, generally higher yields of products were observed in thicker films. These may indicate either more molecules exposed to UV (if film thickness is comparable with UV penetration depth) or molecules more liable to UV modification (if higher molecular mobility is present in thicker films). The effect of the second 8 J/cm^2 UV dose on the same set of samples is presented in Fig. 7(b), showing again the higher yields in amorphous films than in semicrystalline films. However, different from previous 8 J/cm^2 UV irradiation, decarbonylation process started to dominate over acid production. The third exposure of 8 J/cm^2 UV dose to the samples were also carried out and the results are summarized in Fig. 7(c), now showing the dominance of decarbonylation process over acid creation. Although decarbonylation yield is still higher in amorphous samples than their semicrystalline counterparts, the acid yield is very similar in either morphology.

The effect of three sequential 8 J/cm^2 UV exposures is more clearly illustrated by comparing ~140 nm thick

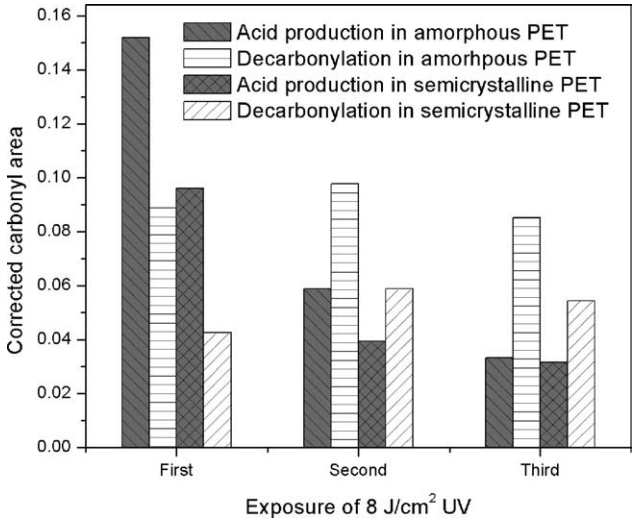

Fig. 8. Effect of three sequential UV exposures, each of 8 J/cm^2, on ~140 nm PET films.

amorphous and semcrystalline samples in Fig. 8. The first 8 J/cm^2 UV resulted in much higher yield of acid than of decarbonylation in both amorphous and semicrystalline. After the second and third 8 J/cm^2 UV exposures, the acid yield diminished quickly while decarbonylation yield remains about the same level. The same is true for samples at other thickness. This decrease of macroscopic quantum yield of acid product can be attributed to the preferential depletion of the more reactive sites in the early stages of the process [36]. This behavior is consistent with inherent conformation selectivity of Norrish type II reaction, whereas decarbonylation process sustained stable quantum yield through 24 J/cm^2 UV.

Learning depth of modification by 172 nm UV irradiation would provide more insight in understanding the increase of photochemical yield in thicker films (Fig. 7). A pair of ~300 nm thick amorphous and semicrystalline films previously exposed to a total UV dose of 24 J/cm^2 were subject to plasma etching and their IR spectra and film thickness were measured after every etching cycle. The residual positive carbonyl band areas (above the linear background extended from lower wavenumber side) in the difference spectra of semicrystalline and amorphous samples were plotted against etching depth in Fig. 9. Both samples showed lower remaining carboxylic band area with increased etching depth and reached a minimum value of ~0.04 after removal of about 100 nm, indicating the majority of the photochemical transformation has occurred within 100 nm surface layer. With this small modified depth, the increase of film thickness beyond ~100 nm will not offer much additional sample to UV exposure. We are, therefore, to attribute the enhanced photochemical reactions in thicker films to higher molecular mobility in material not affected by the strong polymer-substrate interaction adjacent to the interface discussed earlier.

The increase of yield with thickness saturates at about 400 nm, suggesting that films this thick or more represent bulk polymer for our purpose. The average quantum yields

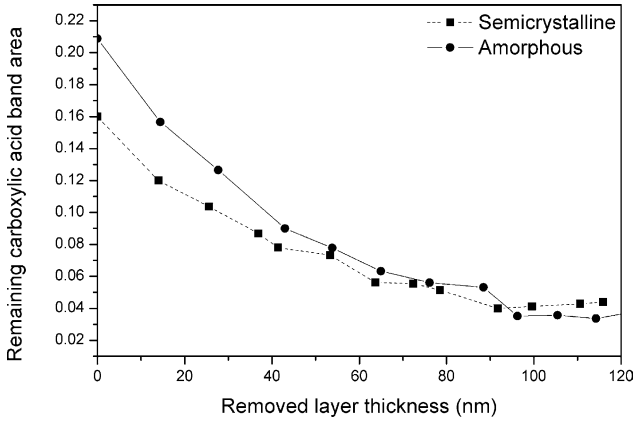

Fig. 9. Residual positive absorbance carbonyl band areas in the difference spectra of 24 J/cm^2 UV modified semicrystalline and amorphous films with respective ~400 nm thick virgin PET films after every plasma etching cycle.

of acid production and decarbonylation for 8 J/cm^2 172 nm UV irradiation in ~400 nm semicrystalline sample were calculated to be 14.3×10^{-4} and 4.6×10^{-4}, respectively. They are very close to the initial quantum yield of Mylar film 17.2×10^{-4} and 6.1×10^{-4}, reported by Day and Wiles [5] at longer UV wavelength (300–420 nm). This agrees very well with Kasha's rule [37], stating only the lowest excited states need to be considered for initiation of photochemical processes and thus quantum yield of particular photochemical process is independent of initial excitation energy.

4. Conclusion

Phototransformation of PET by 172 nm UV irradiation was studied with transmission infrared spectroscopy of spin cast thin films on silicon substrates. The proposed Norrish type I and II photodegradation mechanisms accounted for the difference spectra between UV treated and untreated samples. Quantitative analysis were carried out by simulating carbonyl-stretching band in the difference spectra with ester and acid type carbonyl model spectra. At low dose level (8 J/cm^2), Norrish type II process, forming acid product, dominated over Norrish type I based decarbonylation. *trans* Ethylene glycol conformers were selectively transformed by Norrish type II reaction whereas low selectivity of carbonyl conformations as well as conformers resulting from rotation about the C–O glycol linkage was observed. At higher dose levels, acid production quickly lowered due to the depletion of preferential reaction sites. Lower molecular mobility manifested in the vicinity of polymer-substrate interface inhibited yields of both photochemical processes. Although the yields were lower in semicrytalline films than amorphous ones, no significant difference was observed between amorphous and crystalline phase of the same film. This distinctive behavior suggests that semicrystalline PET is a strongly correlated molecular dynamic system, where photochemical response of both phases was affected by the degree of crystallization. Consistent with this notion, others had to introduce variable densities of both phases to account for the abnormal gas transport behaviors of PET with different crystallinity [38]. Similarly, treating IR spectra of semicrystalline PET as linear combinations of spectra of pure amorphous and crystalline materials also faces some difficulties [21,24]. In addition, depth profiling of 172 nm UV treated samples show a shallow modification depth (~100 nm) so that the UV modification may be expected to have high efficiency in transforming surface properties and little detrimental effect on the bulk.

Acknowledgements

We are grateful for helpful discussions with Dr Dennis J.

Walls of DuPont and Prof Christopher J. Abelt of the College of William and Mary.

References

[1] Chemical and Engineering News 81; 2003.
[2] Day M, Wiles DM. J Appl Polym Sci 1972;16:175–89.
[3] Day M, Wiles DM. J Appl Polym Sci 1972;16:191–202.
[4] Day M, Wiles DM. J Appl Polym Sci 1972;16:203–15.
[5] Day M, Wiles MD. Polym Lett 1971;9:665–9.
[6] Lazare S, Srinivasan R. J Phys Chem 1986;90:2124–31.
[7] Chtaib M, Roberfroid EM, Novis Y, Pireaux JJ, Caudano R, Lutgen P, et al. J Vac Sci Technol A 1989;7:3233–7.
[8] Praschak D, Bahners T, Schollmeyer E. Appl Phys A 1998;66:69–75.
[9] Zhang J, Esrom H, Kogelschatz U, Emig G. J Adhesion Sci Technol 1994;8:1179–210.
[10] Zhu Z, Kelley MJ. Appl Surf Sci 2004;236:416–25.
[11] Zhu Z, Kelley MJ. Appl Surf Sci 2004;231–232:302–8.
[12] Ward IM. Chem Ind 1956;905–6.
[13] Daniels WW, Kitson RE. J Polym Sci 1958;33:161–70.
[14] Miyake A. J Polym Sci 1959;38:479–95.
[15] Miyake A. J Polym Sci 1959;38:497–512.
[16] Krimm S. Adv Polym Sci 1960;2:51–172.
[17] Manley TR, Williams DA. Polymer 1969;10:330–84.
[18] Cunningham A, Ward IM, Willis HA, Zichy V. Polymer 1974;15: 749–56.
[19] Bahl SK, Cornell DD, Boerio FJ, McGraw GE. J Polym Sci, Polym Lett Ed 1974;12:13–19.
[20] Boerio FJ, Bahl SK, McGraw GE. J Polym Sci, Polym Phys Ed 1976; 14:1029–46.
[21] D'Esposito L, Koenig JL. J Polym Sci, Polym Phys Ed 1976;14: 1731–41.
[22] Štokr J, Schneider B, Doskočilová D, Lövy J, Sedláček P. Polymer 1982;23:714–21.
[23] Fina LJ, Koenig JL. Macromolecules 1984;17:2572–9.
[24] Cole KC, Ajji A, Pellerin É. Macromolecules 2002;35:770–84.
[25] de Daubeny RP, Bunn CW, Brown C. J Proc R Soc London 1954; 226A:531–42.
[26] Yamamoto K, Ishida H. Appl Optics 1995;34:4177–85.
[27] Walls DJ. Appl Spectrosc 1991;45:1193–8.
[28] Dunn DS, Ouderkirk AJ. Macromolecules 1990;23:770–4.
[29] Sills S, Overney RM, Chau W, Lee VY, Miller RD, Frommer J. J Chem Phys 2004;120:5334–8.
[30] Buenviaje C, Ge S, Rafailovich M, Sokolov J, Drake JM, Overney RM. Langmuir 1999;15:6446–50.
[31] Kaito A, Kyotani H, Hajiheidari D, Tanigaki N, Shimomura M. Polymer 1999;40:5857–63.
[32] van Zanten JH, Wallace WE, Wu W. Phys Rev E 1996;53:R2053–R6.
[33] Forrest JA, Dalnoki-veress K, Dutcher JR. Phys Rev E 1997;56: 5705–16.
[34] Turro NJ. Modern molecular photochemistry. California: Benjamin/-Cumming; 1978. p. 386–392.
[35] Tonelli AE. J Polym Sci, Polym Lett Ed 1973;11:441–7.
[36] Pitts E, Reiser A. J Am Chem Soc 1983;105:5590–3.
[37] Kasha M. Disc Faraday Soc 1950;9:14–19.
[38] Qureshi N, Stepanov EV, Schiraldi D, Hiltner A, Baer E. J Polym Sci, Part B: Polym Phys 2000;38:1679–86.